Salt Effect on Stability and Solvation Structure of Peptide: An Integral Equation Study

Takashi Imai, Masahiro Kinoshita,† and Fumio Hirata*,††

Department of Functional Molecular Science, The Graduate University for Advanced Studies, Okazaki, Aichi 444-8585

†Advanced Energy Utilization Division, Institute of Advanced Energy, Uji, Kyoto 611-0011

††Department of Theoretical Study, Institute for Molecular Science and Department of Functional Molecular Science, The Graduate University for Advanced Studies, Okazaki, Aichi 444-8585

(Received December 2, 1999)

Salt effects on the stability and on the solvation structure of a peptide in a variety of aqueous solutions of the alkali-halide ions are studied by means of the reference interaction site model (RISM) theory. The order of salt effect on the peptide stability is consistent with the experimental results; the order follows the Hofmeister series. The results are further analyzed in order to clarify the nature of the salt effect which determines the Hofmeister series and to find the reason why the Hofmeister series applies so generally to a variety of solutes in aqueous solutions. A heuristic model for explaining salt effects on the solvation structure of the peptide is proposed based on changes in the peptide–water pair correlation functions due to the ion perturbation.

The stability of protein depends sensitively on some thermodynamic conditions, such as solvent, temperature, pressure, and coexisting solutes. Among those conditions, one of the most extensively studied is salt effects.[1—3] The salt effect on the stability of protein in aqueous solutions is known to follow some order called the Hofmeister series. For anions, the series is

$$SO_4^{2-} > CH_3COO^- > Cl^- > Br^- > NO_3^- > ClO_4^- > I^- > CNS^-,$$

and for cations, it is

$$(CH_3)_4N^+ > NH_4^+ > Rb^+, K^+, Na^+, Cs^+ > Li^+ > Mg^{2+} > Ca^{2+} > Ba^{2+}.$$

In the above series, the species to the left (right) decrease (increase) the solubility of proteins, namely salting-out (salting-in), and stabilize (destabilize) their native structure. It has been shown that the Hofmeister series is generally applied to neutral proteins, but not to acidic or to basic proteins.[4,5] The series, except for divalent cations, is also applied to the other neutral substances such as benzene.[6] In short, the effect of monovalent ions on the solubility of various neutral substances follows the Hofmeister series. It is generally believed that the Hofmeister series is somehow related to the free energy change associated with change in water structure caused by perturbation of ions.[2] If this is the case, how are those two related? What kinds of structural changes in water are responsible for such a sequence of the salt effects? The Hofmeister series is originally found for solubility of protein,[7] but it apparently has some connection with the conformational stability of the biopolymer. Then, what is the relation between salt effects on the two different properties? It is our ultimate goal to answer those questions concerning the salt effect on protein stability.

Such questions may not be answered entirely from experiments. Even for theories, there are many problems to be overcome. The continuum model of electrolyte solutions can not provide any information concerning the structural modification of water, and it does not give a proper account for the associated change in the free energy due to ions. Molecular simulations in the current stage may not produce reliable results for such subtle effects which should take account for small differences in ion species. The methods are notorious for the inefficient sampling of the free energy, and it becomes almost fatal when a multicomponent system is involved due to slow convergence of the diffusion process. The reference interaction site model (RISM) theory in the statistical mechanics of molecular liquids has the potential capability of investigating the problems described above, i.e. molecular pictures of changes in the water structure caused by the addition of salts near a protein and associated changes in the solvation free energy. Nevertheless, the RISM theory has never been applied to analyses on this kind of phenomena, because severe numerical instability was often encountered when one tries to solve the RISM equations for a system including ions and/or a solute with many atomic sites. Recently, Kinoshita et al. developed a robust and extremely efficient algorithm for solving the RISM equations for salt solutions near a solute atom[8] and for pure water near a solute molecule with many atomic sites.[9,10] As an extension, a dipeptide–NaCl solution system has been studied.[11] In the present study, we investigate salt effects on the solvation free energy of a peptide and solvation structures near the peptide in various alkali-halide solutions.

This paper is organized as follows. In the following sec-

tion, we briefly outline the method of calculating the solvation free energy of peptide and the radial distribution functions of solvent species (water and ions) around the solute based on the RISM theory. Section 2 is divided into two subsections, which are devoted to detailed discussions of the results concerning salt effects on the solvation free energy and solvation structures of peptide. Section 3 concludes the paper.

1. Theory

1.1. RISM Theory. For a system consisting of several molecular species, a general expression of the RISM equation (site-site Ornstein–Zernike equation) can be written as,[12–15]

$$\rho\tilde{\boldsymbol{h}}\rho = \tilde{\boldsymbol{\omega}}\tilde{\boldsymbol{c}}\tilde{\boldsymbol{\omega}} + \tilde{\boldsymbol{\omega}}\tilde{\boldsymbol{c}}\rho\tilde{\boldsymbol{h}}\rho, \tag{1}$$

where $\boldsymbol{\rho}$ is the diagonal matrix of number density of molecular species, and $\boldsymbol{h}$, $\boldsymbol{c}$, and $\boldsymbol{\omega}$ are the total, direct, and intramolecular correlation matrices, respectively. Tildes indicate the Fourier transform of those functions. In the case of the infinite dilution limit in which the concentration of the molecular species tends to zero (the species are called solute, the other species are called solvent.), the RISM equation can be decomposed into the solvent–solvent, solute–solvent, and solute–solute equations, namely,

$$\tilde{\boldsymbol{h}}^{\mathrm{vv}} = \tilde{\boldsymbol{w}}^{\mathrm{v}}\tilde{\boldsymbol{c}}^{\mathrm{vv}}(\tilde{\boldsymbol{w}}^{\mathrm{v}} + \boldsymbol{\rho}^{\mathrm{v}}\tilde{\boldsymbol{h}}^{\mathrm{vv}}), \tag{2}$$

$$\tilde{\boldsymbol{h}}^{\mathrm{uv}} = \tilde{\boldsymbol{w}}^{\mathrm{u}}\tilde{\boldsymbol{c}}^{\mathrm{uv}}(\tilde{\boldsymbol{w}}^{\mathrm{v}} + \boldsymbol{\rho}^{\mathrm{v}}\tilde{\boldsymbol{h}}^{\mathrm{vv}}), \tag{3}$$

$$\tilde{\boldsymbol{h}}^{\mathrm{uu}} = \tilde{\boldsymbol{w}}^{\mathrm{u}}\tilde{\boldsymbol{c}}^{\mathrm{uu}}\tilde{\boldsymbol{w}}^{\mathrm{u}} + \tilde{\boldsymbol{w}}^{\mathrm{u}}\tilde{\boldsymbol{c}}^{\mathrm{uv}}\boldsymbol{\rho}^{\mathrm{v}}\tilde{\boldsymbol{h}}^{\mathrm{vu}}, \tag{4}$$

where the superscripts "u" and "v" denote "solute" and "solvent", respectively, and $\tilde{\boldsymbol{w}} = \tilde{\boldsymbol{\omega}}\tilde{\boldsymbol{\rho}}^{-1}$. Those equations are solved with the hypernetted chain (HNC) type of closure equation,

$$c_{\mathrm{ab}}(r) = \exp\left[-u_{\mathrm{ab}}(r)/k_{\mathrm{B}}T + h_{\mathrm{ab}}(r) - c_{\mathrm{ab}}(r)\right] - (h_{\mathrm{ab}}(r) - c_{\mathrm{ab}}(r)) - 1, \tag{5}$$

where the subscripts "a" and "b" indicate the site labels of the molecular species. u_{ab} is the pair potential between sites a and b.

As has been well regarded, the RISM/HNC theory is poor concerning dielectric properties for polar liquid systems. Therefore, we employ the RISM theory improved by Perkyns and Pettitt to assure the dielectric consistency, which is called the DRISM theory.[16,17] The DRISM equations are written as

$$(\rho\tilde{\boldsymbol{h}}\rho - \tilde{\boldsymbol{\chi}}) = (\tilde{\boldsymbol{\omega}} + \tilde{\boldsymbol{\chi}})\tilde{\boldsymbol{c}}(\tilde{\boldsymbol{\omega}} + \tilde{\boldsymbol{\chi}}) + (\tilde{\boldsymbol{\omega}} + \tilde{\boldsymbol{\chi}})\tilde{\boldsymbol{c}}(\rho\tilde{\boldsymbol{h}}\rho - \tilde{\boldsymbol{\chi}}), \tag{6}$$

where $\tilde{\boldsymbol{\chi}}$ is determined by the dielectric constant, dipole moment, and density of solvent. The detail is given in their original paper.[16,17] If we consider the system of infinite dilution limit again, Eq. 6 can be also decomposed into these equations

$$\tilde{\boldsymbol{h}}^{\mathrm{vv}} = (\tilde{\boldsymbol{w}}^{\mathrm{v}} + \tilde{\boldsymbol{D}}^{\mathrm{vv}}\boldsymbol{\rho}^{\mathrm{v}})\tilde{\boldsymbol{c}}^{\mathrm{vv}}(\tilde{\boldsymbol{w}}^{\mathrm{v}} + \boldsymbol{\rho}^{\mathrm{v}}\tilde{\boldsymbol{h}}^{\mathrm{vv}}) + \tilde{\boldsymbol{D}}^{\mathrm{vv}}, \tag{7}$$

$$\tilde{\boldsymbol{h}}^{\mathrm{uv}} = \tilde{\boldsymbol{w}}^{\mathrm{u}}\tilde{\boldsymbol{c}}^{\mathrm{uv}}(\tilde{\boldsymbol{w}}^{\mathrm{v}} + \boldsymbol{\rho}^{\mathrm{v}}\tilde{\boldsymbol{h}}^{\mathrm{vv}}), \tag{8}$$

$$\tilde{\boldsymbol{h}}^{\mathrm{uu}} = \tilde{\boldsymbol{w}}^{\mathrm{u}}\tilde{\boldsymbol{c}}^{\mathrm{uu}}\tilde{\boldsymbol{w}}^{\mathrm{u}} + \tilde{\boldsymbol{w}}^{\mathrm{u}}\tilde{\boldsymbol{c}}^{\mathrm{uv}}\boldsymbol{\rho}^{\mathrm{v}}\tilde{\boldsymbol{h}}^{\mathrm{vu}}, \tag{9}$$

where $\tilde{\boldsymbol{D}} = \boldsymbol{\rho}^{-1}\tilde{\boldsymbol{\chi}}\boldsymbol{\rho}^{-1}$. We have noticed that Eqs. 8 and 9 are identical to Eqs. 3 and 4, respectively.

In the present work, the solute–solvent (water, cation, and anion) correlation functions in the infinite dilution limit are calculated as follows. At first, we obtain the solvent–solvent correlation functions by iteratively solving Eq. 7 with Eq. 5 for salt solution systems without the solute. Next, the solute–solvent correlation functions are calculated by iteratively solving Eq. 8 with Eq. 5, where the function $\tilde{\boldsymbol{w}}^{\mathrm{v}}+\boldsymbol{\rho}^{\mathrm{v}}\tilde{\boldsymbol{h}}^{\mathrm{vv}}$, which has already been obtained from previous step, is part of the input data. These calculations are carried out by using the algorithm developed by Kinoshita et al.[8–11]

1.2. Solvation Free Energy and Salting Coefficient. For a system consisting of solute (m sites), water (V), cation (C), and anion (A), the solvation free energy for the solute molecule $\Delta\mu_{\mathrm{s}}$ is calculated from[18,19]

$$\Delta\mu_{\mathrm{s}} = I_{\mathrm{V}} + I_{\mathrm{A}} + I_{\mathrm{C}}, \tag{10}$$

$$I_{\mathrm{X}} = 4\pi k_{\mathrm{B}}T\sum_{a=1}^{m}\rho_{\mathrm{X}}\int_0^{\infty}\left[\frac{1}{2}h_{a\mathrm{X}}(r)^2 - c_{a\mathrm{X}}(r) - \frac{1}{2}h_{a\mathrm{X}}(r)c_{a\mathrm{X}}(r)\right]r^2\mathrm{d}r, \tag{11}$$

where "X" denotes "V", "C", or "A". I_{V} is a sum of contributions from H and O of water.

The salting coefficient k_S is defined by

$$k_S = \log(S_0/S)/C, \tag{12}$$

where S_0 and S are the solubilities of solute atoms in pure water and in salt solution of molarity C, respectively. S_0/S is approximately given by[8,20]

$$S_0/S = \frac{(\rho_{\mathrm{V}} + \rho_{\mathrm{C}} + \rho_{\mathrm{A}})\exp\left[\Delta\mu_{\mathrm{s}}/k_{\mathrm{B}}T\right]}{\rho_{\mathrm{V}}^0\exp\left[\Delta\mu_{\mathrm{s}}^0/k_{\mathrm{B}}T\right]}, \tag{13}$$

where ρ_{V}^0 is the number density of pure water, and $\Delta\mu_{\mathrm{s}}^0$ denotes the solvation free energy in the case of pure water.

1.3. Models. We choose acetylglycine ethyl ester (AGE) as a subject of our investigation because such a peptide must be the most basic model of protein; besides the experimental salting-out coefficients of the peptide in various salt solutions are available.[21] The conformation is fixed at the *all-trans* form in the present calculations, which is illustrated in Fig. 1. The following two sets of electrolyte solutions were studied in order to examine effects of cations and anions on the solvation free energy of AGE: LiCl, NaCl, and KCl (set 1) for the cation effect, and NaCl, NaBr, and NaI (set 2) for the anion effect. Temperature and salt concentration are fixed at 298.15 K and 1 M (1 M = 1 mol dm^{-3}), respectively. The number density of water[22] and dielectric constants of electrolyte solutions,[8,23] which are the input data according to the prescription of the DRISM theory, are listed in Table 1.

For the site–site pair potential u_{ab}, we employ the standard type one which consists of the Lennard–Jones potential term and the electrostatic interaction term, namely,

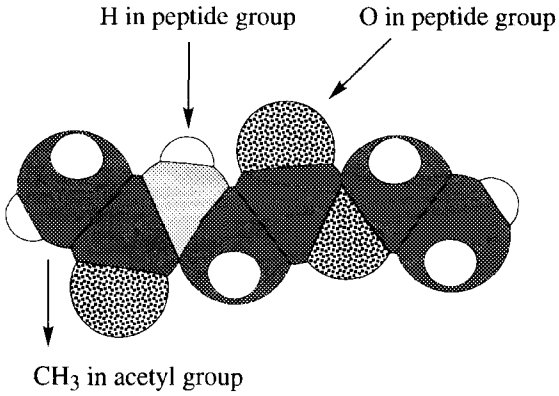

Fig. 1. The structure of acetylglycine ethyl ester (AGE). The three atoms pointed by arrows are selected for discussion of solvation structures of the peptide.

Table 1. The Number Densities of Water (Ref. 22) and Dielectric Constants (Refs. 8 and 23) of the 1 M Salt Solutions

	$\rho_N/\text{Å}^{-3}$	ε
LiCl	0.03269	64
NaCl	0.03269	65
NaBr	0.03247	66
NaI	0.03211	67
KCl	0.03234	67
KBr	0.03212	68
KI	0.03176	69

$$u_{ab}(r) = 4\varepsilon_{ab}\left[\left(\frac{\sigma_{ab}}{r}\right)^{12} - \left(\frac{\sigma_{ab}}{r}\right)^{6}\right] + \frac{q_a q_b}{r}. \quad (14)$$

The standard mixing rules $\varepsilon_{ab} = (\varepsilon_a\varepsilon_b)^{1/2}$ and $\sigma_{ab} = (\sigma_a+\sigma_b)/2$ are employed for calculating the Lennard–Jones potential parameters. The SPC/E model[24] is used for water. The AMBER-type potential parameters are employed for the peptide; these are listed in Table 2. The L–J σ values for the ions were adjusted in a way that the theory qualitatively reproduces the experimental values of the salting-out coefficient of noble gas and the mean activity coefficient in the solutions. (See below.) The σ values are listed in Table 3 along with the corresponding values for ε, which are calculated from the Mavroyannis–Stephan theory.[25,26]

1.4. Determination of Potential Parameter for Ions. There has been no consensus with respect to the potential parameters for ions in water. In our previous study concerning the salt effect on solubility of noble gas in aqueous solutions,[8] we employed the potential parameters for ions based on ones proposed earlier. The RISM theory reproduces the experimental order of the salting-out coefficients for cations, but unfortunately not for anions. Therefore we need to determine a new set of potential parameters for ions. The usual procedure to identify the problem is to determine the potential parameters from the molecular simulation, and then compare the theoretical results for observables with those from the simulation using the same parameters to see if the theory is doing well or not. However, the molecular simulation of electrolyte solutions with explicit solvent molecules is notoriously difficult, and, in particular, reliability of the results for the free energy properties is extremely low. Considering such situations, we take a different approach to study the salt-effect on biomolecules. We first determine a set of interaction parameters for alkali and halide ions, which gives, within the RISM theory, the best fit with experimental results for the activity coefficient of the electrolyte solutions, and for the salting-out coefficients of noble gas (argon) in the solution. Then, the parameter set so determined is used to analyze structural and thermodynamic properties of a peptide solution.

We choose the simplest expression, Eq. 14, for all the inter-

Table 2. Lennard–Jones Potential Parameters and Partial Charges of the Peptide

	σ/2Å	ε/kcal mol^{-1}	Partial charge
($CH_3C{=}O$)			
C	1.60	0.06	−0.142
H	1.37	0.01	0.010
H	1.37	0.01	0.010
H	1.37	0.01	0.010
C	1.65	0.12	0.616
O	1.43	0.20	−0.504
(Gly)			
N	1.56	0.16	−0.463
H	0.89	0.02	0.252
C	1.60	0.06	0.035
H	1.37	0.01	0.032
H	1.37	0.01	0.032
C	1.65	0.12	0.616
O	1.43	0.20	−0.504
(OCH_2CH_3)			
O	1.47	0.15	−0.577
C	1.60	0.06	0.361
H	1.37	0.01	0.100
H	1.37	0.01	0.100
C	1.60	0.06	−0.098
H	1.37	0.01	0.038
H	1.37	0.01	0.038
H	1.37	0.01	0.038

Table 3. Lennard–Jones Potential Parameters for Water and Ions
Numbers in the parentheses are for ion-ion pairs.

	σ/Å	ε/kcal mol^{-1}
H	0.40	0.046
O	3.16	0.156
Li^+	1.48 (1.63)	0.125 (0.070)
Na^+	1.90 (1.86)	0.293 (0.333)
K^+	2.84 (2.67)	0.297 (0.431)
Cl^-	3.62 (3.71)	0.448 (0.387)
Br^-	3.92 (4.04)	0.638 (0.532)
I^-	4.40 (4.54)	0.722 (0.598)

action potentials between ion–ion, ion–water, and ion–solute atomic pairs. The use of the potential function may be oversimplified, because ion–induced dipole and dipole–induced dipole interaction and chemical interaction are not taken into consideration. However, we suppose that such interactions can be buried in the potential parameters to a certain extent. We assume that the parameters of ions for ion–solute interaction are identical with those for ion–water interaction. Based on those assumptions, we determine the L–J σ of ions for ion–water, ion–solute, and ion–ion interactions following the procedure stated above. L–J ε are calculated from L–J σ, ion polarizability, and the total number of electrons of ion using the Mavroyannis–Stephan theory.[25,26] The L–J σ so determined are listed in Table 3 along with ε. Detailed discussion is provided in Ref. 38.

2. Results and Discussion

2.1. Solvation Free Energy of a Peptide. The solvation free energies of acetylglycine ethyl ester (AGE) and the salting-out coefficients are summarized in Table 4, along with the various components defined by Eqs. 10 and 11, and by

$$\chi = I_V - \Delta\mu_s^0, \tag{15}$$

where $\Delta\mu_s^0$ is the solvation free energy of the solute in pure water. The corresponding experimental data[21] are also exhibited in the same table. I_C and I_A are the contributions from the 'direct' ion–solute interactions. Here, by 'direct' ion–solute interaction we do not mean the bare ion–solute interaction described by Eq. 14, but the contribution to the solvation free energy of solute from ions as indicated explicitly in Eq. 11. χ signifies the contributions to solvation free energy from changes in water structure due to the existence of ions. $\Delta\Delta\mu_s$ is defined by

$$\begin{aligned}\Delta\Delta\mu_s &= \Delta\mu_s - \Delta\mu_s^0 \\ &= \chi + I_C + I_A,\end{aligned} \tag{16}$$

which is the difference of the solvation free energy in the electrolyte solutions from that in pure water. It can be readily seen that the order of k_s is consistent with the experimental result, which is nothing but the Hofmeister series. It is worthwhile to decompose the effect into the hydrophobic and charge effects. For that purpose, we have calculated the solvation free energy of an imaginary peptide which is made up from AGE by removing all the partial charges. The solvation free energies for the imaginary peptide, which can be called the 'hydrophobic effect', are summarized in Table 5 along with their components, where superscript "(0)" symbolizes the hydrophobic effect. We define the charge effect by the differences of the free energies between the imaginary peptide and the real peptide, i.e. $X^{(q)} = X - X^{(0)}$, which are shown in Table 6.

Comparing $\Delta\Delta\mu_s^{(0)}$ in Table 5 with $\Delta\Delta\mu_s^{(q)}$ in Table 6, it is readily seen that the charge effect is small in comparison with the hydrophobic effect due to cancellation among $\chi^{(q)}$, $I_C^{(q)}$, and $I_A^{(q)}$. Although ions give influence both on the hydrophobic hydration and the electrostatic effect of solute, the effect on the hydrophobic hydration dominates over the electrostatic effect as a consequence of large cancellations among the electrostatic effects. This implies that the overall salt effect does not depend too much on the electrostatic characteristics of solute, namely, whether the solute has partial charges or not, and how the partial charges are distributed among atoms. As we stated in the introduction, the Hofmeister series applies to a rather wide class of neutral

Table 5. The Solvation Free Energies of the Imaginary Peptide in Which All Site Charges are Removed (Unit in kcal mol^{-1})

	$I_V^{(0)}$	$\chi^{(0)}$	$I_C^{(0)}$	$I_A^{(0)}$	$\Delta\mu_s^{(0)}$	$\Delta\Delta\mu_s^{(0)}$
LiCl	50.74	−0.60	−0.55	1.33	51.53	0.19
NaCl	50.97	−0.37	−0.41	1.33	51.88	0.55
KCl	50.36	−0.97	−0.08	1.31	51.60	0.26
NaCl	50.97	−0.37	−0.41	1.33	51.88	0.55
NaBr	50.66	−0.67	−0.42	1.37	51.62	0.28
NaI	50.23	−1.11	−0.41	1.55	51.36	0.03

Table 6. The Effect of Charges on the Solvation Free Energies of Peptide in Various Salt Solutions (Unit in kcal mol^{-1})

	$\chi^{(q)}$	$I_C^{(q)}$	$I_A^{(q)}$	$\Delta\Delta\mu_s^{(q)}$
LiCl	1.33	−1.79	0.48	0.01
NaCl	1.10	−1.55	0.48	0.03
KCl	0.84	−1.19	0.46	0.11
NaCl	1.10	−1.55	0.48	0.03
NaBr	1.17	−1.56	0.42	0.02
NaI	1.26	−1.58	0.34	0.02

Table 4. The Solvation Free Energies (kcal mol^{-1}) and the Salting-Out Coefficients of AGE in Various Salt Solutions

	I_V	χ	I_C	I_A	$\Delta\mu_s$	$\Delta\Delta\mu_s$	k_s	k_s[expt][a]
LiCl	32.92	0.73	−2.34	1.81	32.39	0.20	0.16	0.10
NaCl	32.92	0.73	−1.96	1.81	32.77	0.58	0.43	0.16
KCl	32.06	−0.13	−1.27	1.77	32.56	0.37	0.28	0.15
NaCl	32.92	0.73	−1.96	1.81	32.77	0.58	0.43	0.16
NaBr	32.69	0.50	−1.98	1.79	32.49	0.30	0.23	0.11
NaI	32.34	0.15	−1.99	1.89	32.24	0.05	0.03	0.04

a) Ref. 21.

solutes. The dominative effect on the hydrophobic hydration can be the reason why the series is so generally applied.

Although it is not entirely clear at the moment why such large cancellation occurs among the electrostatic effects, one possible explanation is provided in terms of 'screening' of the Coulomb interactions. In general, the electrostatic interaction between a pair of ions, repulsive or attractive, is weakened by polar media. The phenomenon, which can be called 'screening', is due to the polarization of solvent by the electrostatic field of ions. The most popular example of such 'screening' effects is the ion–ion Coulomb interaction weakened (or 'divided') by the macroscopic dielectric constant. In the present case, the rather 'direct' electrostatic interaction ($I_C^{(q)}+I_A^{(q)}$) between partial charges of the peptide atoms and the ions could have been 'screened' by the polarization or the reorganization of solvent, which is represented by $\chi^{(q)}$.

We have seen above that the Hofmeister series is dominated by the hydrophobic effect, or $\Delta\Delta\mu_s^{(0)}$. Then, how is the series determined by those contributions to $\Delta\Delta\mu_s^{(0)}$, namely, the contributions from solvent reorganization ($\chi^{(0)}$), the 'direct' effects ($I_C^{(0)}$, $I_A^{(0)}$) of ions? Those contributions are plotted against the salt series in Fig. 2 along with the overall hydrophobic effect, $\Delta\Delta\mu_s^{(0)}$. For the series of anions, the solvent reorganization effect, $\chi^{(0)}$, decreases with the size of anions, while the 'direct' effect, $I_A^{(0)}$ shows the opposite trend. The overall effect is determined essentially by the solvent reorganization effect, because the rate of decrease in $\chi^{(0)}$ is much greater than that of increase in $I_A^{(0)}$. For the series of cations, $\chi^{(0)}$ shows the order $Na^+ > Li^+ > K^+$, while $I_C^{(0)}$ increases with the cation size. Although the overall effect $\Delta\Delta\mu_s^{(0)}$ reflects the order of $\chi^{(0)}$, the order between Li^+ and K^+ reverses due to the effect from $I_C^{(0)}$. Those can be summarized as follows. The Hofmeister series is determined by a balance between the effect on the solvent reorganization and the 'direct' contribution of ions. For anions, the Hofmeister series is dominated by the effect on the solvent reorganization due to ions, while the two effects give comparative contributions for the series of cations.

2.2. Structure of Solvent Near a Peptide. The distribution of solvent (water, cation, and anion) near peptide is complicated by many factors including water–water, ion–ion, ion–water, peptide–water, peptide–ion interactions, and by couplings among those interactions. It will be instructive to summarize earlier conclusions[8,27,28] regarding the ion-hydration before going to the detailed explanation of the results.

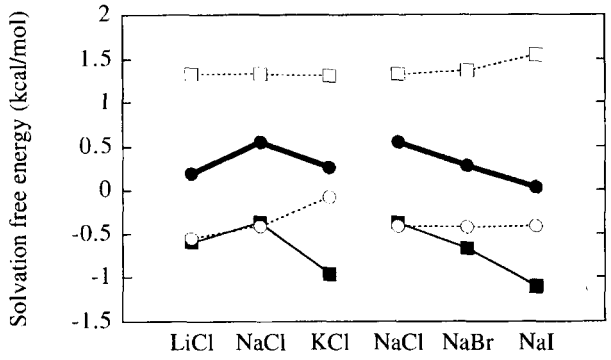

Fig. 2. The contributions to the hydrophobic effect ($\Delta\Delta\mu_s^{(0)}$) from solvent reorganization ($\chi^{(0)}$), and the 'direct' effects of cations ($I_C^{(0)}$) and anions ($I_A^{(0)}$). ●, $\Delta\Delta\mu_s^{(0)}$; ■, $\chi^{(0)}$; ○, $I_C^{(0)}$; □, $I_A^{(0)}$.

First of all, the radial distribution functions (RDF) of water molecules in neat liquid have features which manifest the hydrogen-bond network. The RDF between oxygen and hydrogen has a distinct peak at ca. 1.8, which is assigned to the hydrogen-bond. The oxygen-oxygen RDF has a second peak at the separation around 1.63σ, where σ is diameter of a molecule, which is characteristics of the ice-I-like tetrahedral coordination, and is regarded as the finger print of water structure. The first peak of the O–O RDF is rather sharp, reflecting the much lower coordination number compared to simple liquids. Water-ion interactions are grouped into three categories depending on the ion size and charges. Small monovalent cations and anion, such as Li^+ and Na^+, and F^-, respectively, bind water molecules firmly, which give a well-defined first peak in the ion-water RDF. Those ions are categorized as those of *positive* hydration. The ions give the following perturbations to the water–water RDFs: (1) a decrease in the distribution right at the contact distance associated with an increase in the distribution at slightly further distance, which causes the first peak of the O–O RDF to outward-shift, (2) the second peak of O–O RDF reduces, and (3) the first peak of O–H RDF reduces. On the other hand, water molecules around larger cations and anions such as K^+, Rb^+, Cs^+, and Cl^-, Br^-, respectively, are more disordered or more mobile than those in bulk, which give less distinct first peaks in the ion–water RDFs. The ion–water interactions are called *negative* hydration. The perturbations due to those ions on the water-water RDFs feature (1) inward shift of the O–O first peak, (2) reduction of the O–O second peak, and (3) reduction of O–H first peak. 'Uncharged ions' or non–polar solutes gives different perturbations to the water–water RDF from those of ions: (1) increase in the O–O first peak, (2) decrease in the second peak, (3) increase in the O–H first peak. Those are regarded as a manifestation of the *hydrophobic* hydration. Those characteristics of solute perturbation on the water–water RDF are summarized in Table 7.

The RDF between an ion and nonpolar solute in water has the following feature. The *positively* hydrated ions such as Li^+, Na^+, and F^- have a stable hydration shell which prevents ions from accessing to the solute. On the other

Table 7. Characteristics of Ion Perturbation to Water Structure (Ref. 28)

	Positive hydration	*Negative* hydration	*Hydrophobic* hydration
O–O first peak	$\Longrightarrow$	$\Longleftarrow$	+
O–O second peak	−	−	−
O–H first peak	−	−	+

$\Longrightarrow$: outward shift, $\Longleftarrow$: inward shift, +: peak increases, −: peak decreases.

hand, the *negatively* hydrated ions such as K^+ and Cl^-, Br^- do not have stable hydration shells so that they can access into contact position with the non-polar solute.

Actual distributions of water molecules and ions around a peptide atom is further complicated by the existence of other atoms in the peptide, or the volume exclusion effect, and the electrostatic interactions between charge-peptide groups and solvent (water molecules and ions). As a rule of thumb, the charged groups in a peptide are well exposed to solvent, while the non-polar groups are less exposed and sterically hindered by other peptide atoms from accessing to solvent.

Now we are ready to interpret our results of the RDFs. Three typical peptide-atoms, H of peptide NH group, O of peptide C=O group, and C (CH_3 group) of N-terminal acetyl group (Fig. 1), are chosen for the purpose based on their partial charges: H and O have positive and negative partial charges, respectively, and CH_3 group is essentially neutral.

2.2.1. Peptide NH Group. The RDFs of water oxygen and hydrogen around the hydrogen of NH group in the peptide-bond are plotted in Fig. 3(A). The NH group is sterically protected from solvent access by surrounding atoms. Therefore, the distribution of water molecules and ions around the group is relatively low. However, the RDFs have some distinct features due to the electrostatic interaction between the solvent molecules (water and ions) and the peptide atoms which have rather high partial charges. Since the group is positively charged, it is primarily solvated by the water oxygen, which is apparent from the distinct first peak in the RDFs between water oxygen and peptide hydrogen. The hydrogen atoms are not in contact with the peptide atoms and direct outward from the group.

The cations Li^+, Na^+, and K^+ are electrostatically repelled from the peptide group, and do not have distinct feature in the RDFs (Fig. 3(B)).

The anions Cl^-, Br^-, and I^- are electrostatically attracted by the peptide hydrogen (Fig. 3(C)). The ions are not associated by the strong hydration shell, and are primarily in contact with the peptide hydrogen. The order of the first peak positions are in consent with the distance of the closest approach between the hydrogen and the anions.

2.2.2. Peptide C=O Group. The oxygen of the peptide C=O group is strongly hydrogen-bonded with water molecules, as can been readily seen from Fig. 4(A).

The cations are also bound strongly by the peptide oxygen due to the electrostatic interactions (Fig. 4(B)). The first peak becomes more prominent as the ion size decreases. This can be interpreted as follows. *Positively* hydrated ions such as Li^+ and Na^+ have relatively stable hydration shells. Therefore, a configuration, C=O–water–cation, can be potentially a stable one, which will appear in the RDF as the second peak. The configuration competes with the primarily stable configuration, C=O–cation–water. As the ion size becomes less, the C=O–cation–water becomes dominative over C=O–water–cation configuration.

The anions Cl^-, Br^-, and I^- are expected to be electrostatically repelled by the peptide oxygen. However, the configuration corresponding to the oxygen-anion contact is apparently stabilized (Fig. 4(C)), due maybe to the same reason as seen in the Cl^-–Cl^- PMF in water. Pettitt and Rossky have observed net stabilization of the contact Cl^-–Cl^- pair in water in their theoretical study based on the RISM theory.[29] The essential cause of the net stabilization seems to be the positively-charged hydrogen-atoms of water molecules, which bridge the Cl^-–Cl^- pair. The interesting finding has motivated succeeding studies using the molecular simulations, and has created a controversy regarding whether the net stabilization has real physical sense or not.[30–36] The controversy

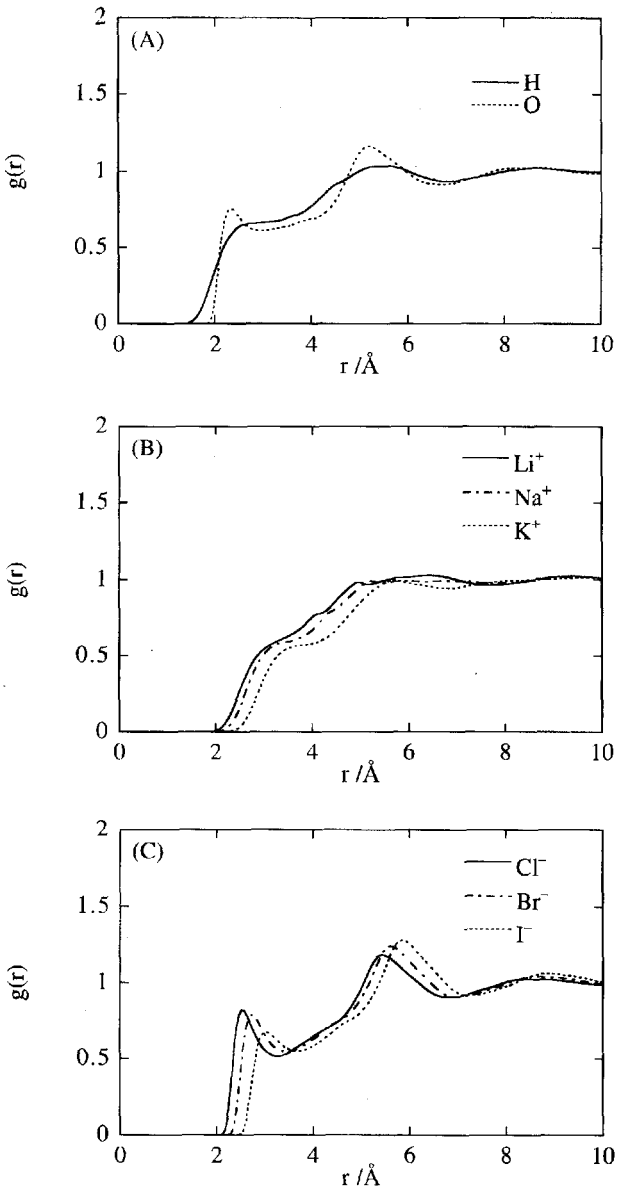

Fig. 3. Solvation structure around the hydrogen atom in the peptide NH group. (A) solid line, H(peptide)–H-(water) in pure water; dotted line, H(peptide)–O(water) in pure water. (B) solid line, H(peptide)–Li^+ in LiCl solution; dot-dashed line, H(peptide)–Na^+ in NaCl solution; dotted line, H(peptide)–K^+ in KCl solution. (C) solid line, H(peptide)–Cl^- in NaCl solution; dot-dashed line, H(peptide)–Br^- in NaBr solution; dotted line, H(peptide)–I^- in NaI solution.

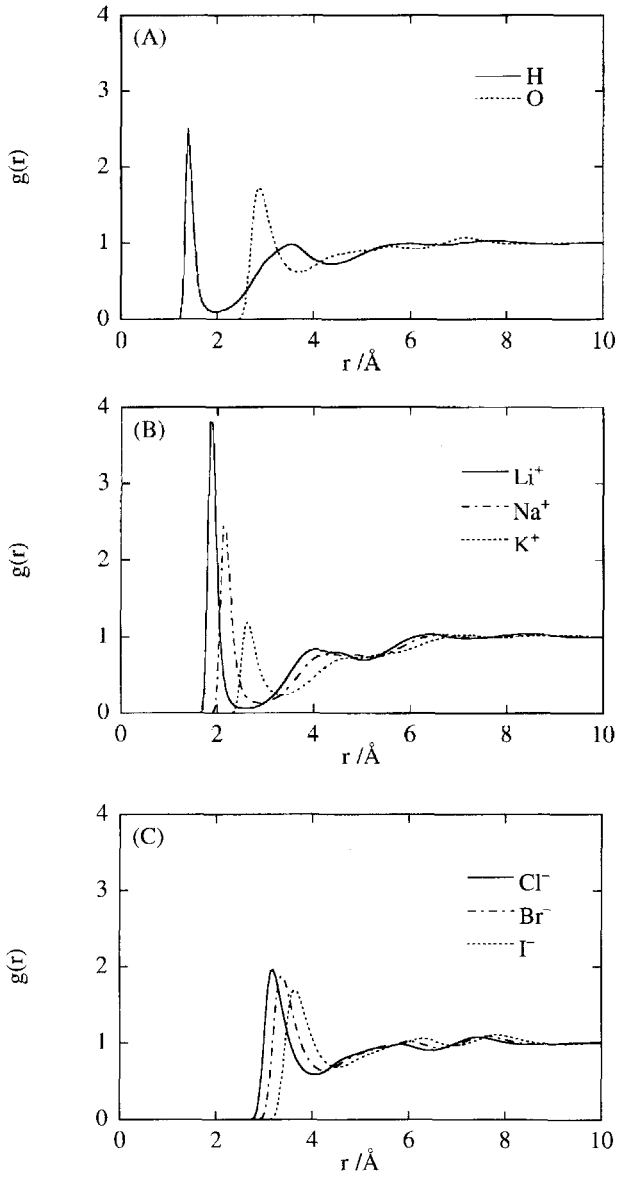

Fig. 4. Solvation structure around the oxygen atom in the peptide C=O group. (A) solid line, O(peptide)–H(water) in pure water; dotted line, O(peptide)–O(water) in pure water. (B) solid line, O(peptide)–Li^+ in LiCl solution; dot-dashed line, O(peptide)–Na^+ in NaCl solution; dotted line, O(peptide)–K^+ in KCl solution. (C) solid line, O(peptide)–Cl^- in NaCl solution; dot-dashed line, O(peptide)–Br^- in NaBr solution; dotted line, O(peptide)–I^- in NaI solution.

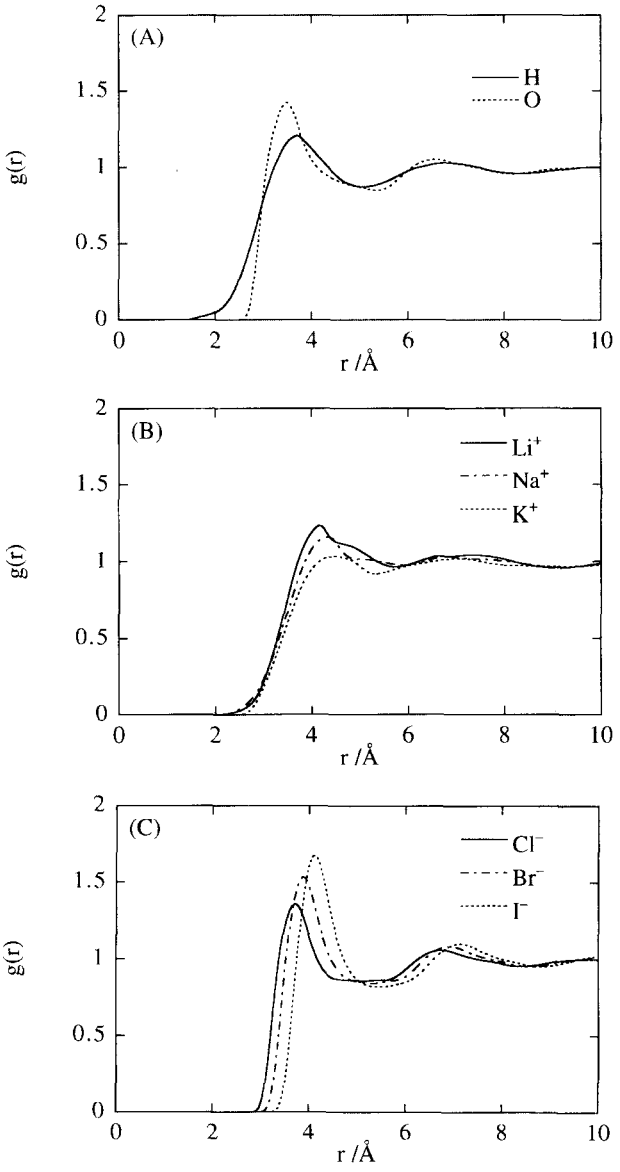

Fig. 5. Solvation structure around the methyl group in the N-terminal acetyl group. (A) solid line, C(methyl)–H(water) in pure water; dotted line, C(acetyl)–O(water) in pure water. (B) solid line, C(methyl)–Li^+ in LiCl solution; dot-dashed line, C(methyl)–Na^+ in NaCl solution; dotted line, C(methyl)–K^+ in KCl solution. (C) solid line, C(methyl)–Cl^- in NaCl solution; dot-dashed line, C(methyl)–Br^- in NaBr solution; dotted line, C(methyl)–I^- in NaI solution.

has not been resolved to date.

2.2.3. CH_3 Group. The RDFs of water oxygen and hydrogen around the CH_3 in N-terminal acetyl group are plotted in Fig. 5(A). They are similar to that around the nonpolar solute.[8]

The cations Li^+, Na^+, and K^+ do not show any distinct feature in the RDFs (Fig. 5(B)).

The RDFs of the anions Cl^-, Br^-, and I^- (Fig. 5(C)) also present similar features to the case for the nonpolar solute[8] as follows. The first peak becomes higher as the anion size increases. Because the anions are hydrated more stably in the order $Cl^- > Br^- > I^-$, they come into contact with the solute site more favorably in the order $Cl^- < Br^- < I^-$.

2.3. Salt Effects on Peptide–Water Distribution. Here, we define the change in the solvation structure around peptide-atoms due to salt effects by

$$\Delta g(r) = \text{“}g(r) \text{ in salt solution”} - \text{“}g(r) \text{ in water”}, \tag{17}$$

where “$g(r)$ in salt solution” denotes the RDF between peptide and water atoms in salt solution, and “$g(r)$ in water” is

that in pure water.

It is convenient to classify the salt effect on the peptide–water RDF into three categories. The first of those is related to the *positively* hydrated ions discussed in the previous subsection, which bind water molecules rather firmly. The *positively* hydrated ions cause $\Delta g(r)$ either positive or negative change depending on charges of the ion and the peptide atom. When charges of the ion and the peptide-atom have opposite signs, $\Delta g(r) > 0$, because the ion brings the associated water molecule into closer contact with the peptide atom. On the other hand, $\Delta g(r) < 0$, if charges of the ion and atom have the same sign, because the ion takes the associated water molecules away from the peptide atom. We call this effect 'positive hydration effect'. The second effect is due to the *negative* hydration described also in the previous subsection. The effect gives rise to positive $\Delta g(r)$, because the *negative* hydration causes the water configuration around the peptide atom to become more packed and denser, because the ice-like open packed structure is disrupted due to ion perturbation. We refer to this as 'negative hydration effect'. The last effect to be considered is due to replacement of a water molecule at contact to the peptide by the ion itself. This occurs when the contact ion–peptide configuration is more stable than that between water and peptide, and it causes $\Delta g(r)$ to be negative due to obvious reasons. We call it 'ion-exchange effect'. The effect will become important when the ion and the peptide atom have opposite charges.

2.3.1. Peptide NH Group–Water. In Fig. 6, plotted are $\Delta g(r)$ for the H(peptide)–O(water) pair. The H(peptide) features positive partial charge (Table 2). Figure 6(A) focuses basically on the difference of the cation effect, but it is necessary to take the effect from Cl^- into account as a common background. We may expect the 'negative hydration effect' for Cl^-, because the ion is known as a *negatively* hydrated ion. Since the 'negative hydration effect' give rise to positive contribution to $\Delta g(r)$, we expect some positive change in the H(peptide)–O(water) RDF as a background. Li^+ and Na^+ are classified as *positively* hydrated ions in the order $Li^+ > Na^+$ for the strength of binding water molecules. The cations are electrostatically repelled from H(peptide), thereby those ions are expected to cause a negative contribution to $\Delta g(r)$ ('positive hydration effect'), which are in competition to the contribution from Cl^-. The figure indicates that the 'positive hydration effect' of cation is dominative for Li^+, while the 'negative hydration effect' due to Cl^- surpasses the 'positive hydration effect' of the cation for Na^+. K^+ is classified as a *negatively* hydrated ion, therefore it gives the same effect as Cl^- giving rise to large positive contribution to $\Delta g(r)$.

Figure 6(B) shows the difference of the anion effect. For anion, the 'negative hydration effect' is dominant as described above. The effect is expected to be in the order $Cl^- < Br^- < I^-$ because the effect increases as the ion gets larger.[37]

2.3.2. Peptide C=O Group–Water. $\Delta g(r)$ for the O(peptide)–H(water) pair is plotted in Fig. 7. In the case shown in Fig. 7(A), Cl^- as a common anion makes $\Delta g(r) > 0$ by the 'negative hydration effect'. The cations, Li^+, Na^+, and K^+, come preferably into the contact position to the O(peptide) atom rather than solvent-separated position as has been clarified in Fig. 4(B). Therefore, the cations cause negative contribution to $\Delta g(r)$ due to the 'ion-exchange effect', in the order $Li^+ > Na^+ > K^+$. The figure indicates that the 'negative hydration effect' of Cl^- dominates in the case of KCl, while the 'ion-exchange effect' of cations surpasses in the cases of LiCl and NaCl.

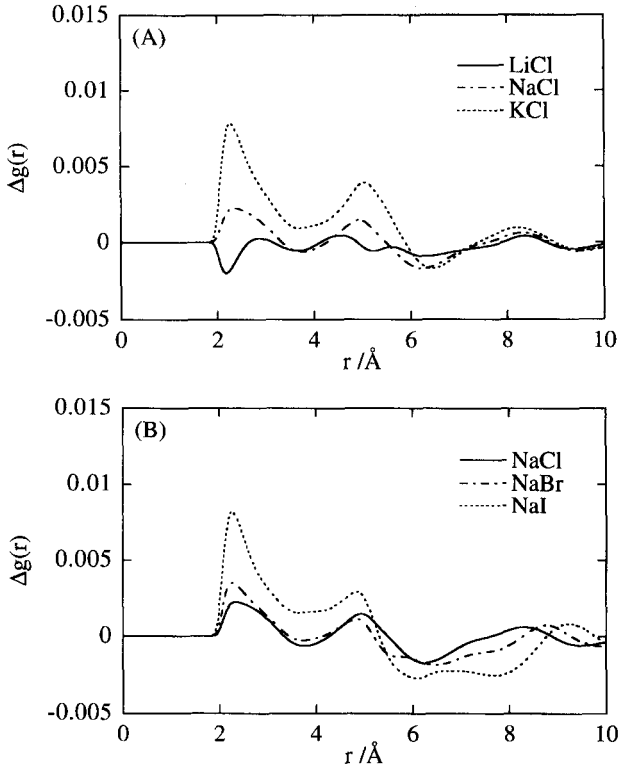

Fig. 6. Change in the water structure around the hydrogen atom in the peptide NH group due to salt effects. (A) solid line, H(peptide)–O(water) in LiCl solution; dot-dashed line, H(peptide)–O(water) in NaCl solution; dotted line, H(peptide)–O(water) in KCl solution. (B) solid line, H(peptide)–O(water) in NaCl solution; dot-dashed line, H(peptide)–O(water) in NaBr solution; dotted line, H(peptide)–O(water) in NaI solution.

Figure 7(B) can be interpreted similarly. Na^+ decreases H(water) population around the O(peptide) atom due to the 'ion-exchange effect' as a back ground. The anions give positive contributions to $\Delta g(r)$ by the 'negative hydration effect' in the order $Cl^- < Br^- < I^-$. The 'negative hydration effect' exceeds in the case of NaI, while the 'ion-exchange effect' dominates in the case of NaCl. The two effects are balanced in the case of NaBr.

3. Summary

Salt effects on the stability and on the solvation structure of a peptide in a variety of aqueous solutions of the alkali-halide ions have been studied by means of the reference interaction site model (RISM) theory.

The order of salt effect on the peptide stability is found to be consistent with the experimental results, which follows the

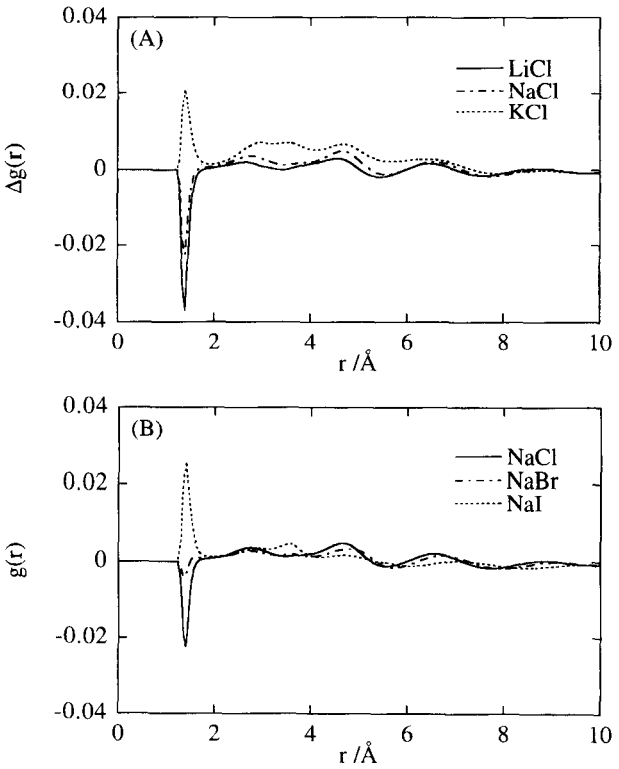

Fig. 7. Change in the water structure around the oxygen atom in the peptide C=O group due to salt effects. (A) solid line, O(peptide)–H(water) in LiCl solution; dot-dashed line, O(peptide)–H(water) in NaCl solution; dotted line, O(peptide)–H(water) in KCl solution. (B) solid line, O(peptide)–H(water) in NaCl solution; dot-dashed line, O(peptide)–H(water) in NaBr solution; dotted line, O(peptide)–H(water) in NaI solution.

Hofmeister series. Salt effects on the solvation free energy of the peptide have been analyzed by decomposing those into the hydrophobic and charge effects. Each of them has been further decomposed into the contributions from changes in water structure due to the existence of ions and from the 'direct' ion–solute interactions. From the analysis, we have drawn the following conclusions for the salt effect. Salts give effect on both the hydrophobic hydration and the electrostatic interaction. However, effects on the electrostatic interaction largely cancel out, and the salt effects on the hydrophobic hydration become dominative. We believe this is the reason why the Hofmeister series applies rather generally to the salt effect on a wide variety of solutes including protein. The Hofmeister series is determined by competition between the order of salt effect through the structural reorganization of water and that of the 'direct' ion–solute interaction. For anions, the former dominates the latter, and the Hofmeister series is determined exclusively by the order of salt effect through the structural reorganization of water. The two effects give comparative contributions for the series of cations.

The salt effect on solvation structure of the peptide atoms has been analyzed extensively in terms of changes in the peptide–water pair correlation functions due to perturbation from ions. We have proposed heuristic interpretations for salt effects on the radial distribution functions between peptide and water atoms based on the well-regarded experimental concepts of ion hydration: 'positive hydration', 'negative hydration', and 'ion-exchange' effects. The complicated effects involving interactions among peptide, water and ions have been interpreted in a consistent manner in terms of the heuristic model.

In the present study, we did not attempt to clarify relations between salt effects on the solvation structure and on the stability of peptide. Such study will require detailed analysis of the effect of salts on the solvation free energy and its decomposition to entropy and enthalpy contributions. There is another important question which we have not answered in the present study: How is the salt effect on solubility of peptides related to that on their conformational stability? The studies to answer those questions are now in progress in our group.

The authors are grateful to Prof. Y. Goto for stimulating discussions which have motivated the present study. The work is supported by a grant from "Research for the Future" Program (Project No. JSPS-RFTF 98P01101) of the Ministry of Education, Science, Sports and Culture.

References

1 P. H. von Hippel and T. Schleich, "Structure and Stability of Biological Macromolecules," ed by S. N. Timasheff and G. D. Fasman, Marcel Dekker, New York (1969), p. 417.

2 K. I. Collins and M. W. Washabaugh, *Q. Rev. Biophys.*, **18**, 323 (1985).

3 R. L. Baldwin, *Biophys. J.*, **71**, 2056 (1996).

4 M. Ries-Kautt and A. Ducruix, *Methods Enzymol.*, **276**, 23 (1997).

5 Y. Goto, N. Takahashi, and A. L. Fink, *Biochemistry*, **29**, 3480 (1990).

6 W. F. McDevit and F. A. Long, *J. Am. Chem. Soc.*, **74**, 1773 (1952).

7 F. Hofmeister, *Arch. Exp. Pathol. Pharmakol.*, **24**, 247 (1888).

8 M. Kinoshita and F. Hirata, *J. Chem. Phys.*, **106**, 5202 (1997).

9 M. Kinoshita, Y. Okamoto, and F. Hirata, *J. Comput. Chem.*, **18**, 1320 (1997).

10 M. Kinoshita, Y. Okamoto, and F. Hirata, *J. Chem. Phys.*, **107**, 1586 (1997).

11 M. Kinoshita, Y. Okamoto, and F. Hirata, *J. Comput. Chem.*, **19**, 1724 (1998).

12 D. Chandler and H. C. Andersen, *J. Chem. Phys.*, **57**, 1930 (1972).

13 F. Hirata and P. J. Rossky, *Chem. Phys. Lett.*, **83**, 329 (1981).

14 F. Hirata, B. M. Pettitt, and P. J. Rossky, *J. Chem. Phys.*, **77**, 509 (1982).

15 F. Hirata, P. J. Rossky, and B. M. Pettitt, *J. Chem. Phys.*, **78**, 509 (1983).

16 J. Perkyns and B. M. Pettitt, *Chem. Phys. Lett.*, **190**, 626 (1992).

17 J. Perkyns and B. M. Pettitt, *J. Chem. Phys.*, **97**, 7656 (1992).

18 S. J. Singer and D. Chandler, *Molec. Phys.*, **55**, 621 (1985).

19 D. A. Zichi and P. J. Rossky, *J. Chem. Phys.*, **84**, 5020 (1986).
20 W. L. Masterton and T. P. Lee, *J. Phys. Chem.*, **74**, 2809 (1970).
21 P. K. Nandi and D. R. Robinson, *J. Am. Chem. Soc.*, **94**, 1308 (1972).
22 J. D'Ans, H. Surawski, and C. Synowietz, "Densities of Binary Aqueous Systems and Heat Capacities of Liquid Systems," ed by Kl. Schäfer, Springer, Berlin (1977), Landolt–Börnstein, IV/1b.
23 H. Behret, F. Schmithals, and J. Barthel, *Z. Phys. Chem.*, **96**, 73 (1975).
24 H. J. C. Berendsen, J. R. Grigera, and T. P. Straatsma, *J. Phys. Chem.*, **91**, 6269 (1987).
25 C. Mavroyannis and M. J. Stephen, *Molec. Phys.*, **5**, 629 (1962).
26 W. L. Masterton, D. Bolocofsky, and T. P. Lee, *J. Phys. Chem.*, **75**, 2809 (1971).
27 S.-H. Chong and F. Hirata, *J. Phys. Chem. B*, **101**, 3209 (1997).
28 F. Hirata, *Bull. Chem. Soc. Jpn.*, **71**, 1483 (1998).
29 B. M. Pettitt and P. J. Rossky, *J. Chem. Phys.*, **84**, 5836 (1986).
30 L. X. Dang and B. M. Pettitt, *J. Am. Chem. Soc.*, **109**, 5531 (1987).
31 L. X. Dang and B. M. Pettitt, *J. Chem. Phys.*, **84**, 6560 (1987).
32 L. X. Dang, B. M. Pettitt, and P. J. Rossky, *J. Chem. Phys.*, **96**, 4046 (1992).
33 E. Guardia, R. Rey, and J. A. Padro, *Chem. Phys.*, **155**, 187 (1991).
34 E. Guardia, R. Rey, and J. A. Padro, *J. Chem. Phys.*, **95**, 2823 (1991).
35 G. Hummer and D. M. Soumpasis, *Mol. Phys.*, **75**, 633 (1992).
36 G. Hummer, D. M. Soumpasis, and M. Neumann, *Mol. Phys.*, **81**, 1155 (1993).
37 O. Ya. Samoilov, "Water and Aqueous Solutions: Structure and Thermodynamics, and Transport Processes," ed by R. A. Horne, Wiley-Interscience, New York (1972), p. 597.
38 T. Imai, Ph.D. Thesis, Grad. Univ. Advanced Studies, 1999.